REVISTA INTERDISCIPLINAR DE PESQUISA EM ENGENHARIA

CILAMCE 2016

XXXVII IBERIAN LATIN AMERICAN CONGRESS ON COMPUTATIONAL METHODS IN ENGINEERING
BRASÍLIA - DF - BRAZIL

ANALYSIS OF ACOUSTIC WAVEGUIDE THROUGH THE ENERGY SPECTRAL ELEMENT METHOD INCLUDING PARAMETERS UNCERTAINTY

Elson C. Moraes

Vilson S. Pereira

Dalmo I. G. Costa

elson.cm@ufma.br

vilson.sp@ufma.br

dalmo.costa@ufma.br

Federal University of Maranhão

Avenida dos Portugueses, 1966 Bacanga, São Luís - MA, 65080-805.

Marcela R. Machado

marcelam@unb.br

University of Brasilia

Engineering Mechanics Department - Bloco G Sala 1-19/8 Faculdade de Tecnologia, 70910-900, Brasilia-DF, Brazil.

José Maria C. Dos Santos

zema@fem.unicamp.br

University of Campinas

Computational Mechanics Department, Faculty of Mechanical Engineer, State University of Campinas-UNICAMP, 13083-970,Campinas-SP, Brazil.

Abstract. *Sound field behaviour in an acoustic enclosure is an important part of the cabin passenger transport vehicle design, concert halls, conference rooms, etc., different analytical methods are available to design engineers, which has its strengths and weaknesses. Cavities in a low-frequency band and negligible absorption on the walls can be modelled by Modal Analysis and Finite Element Method. However, when the frequency band increases, both methods become computationally expensive and Statistical Energy Analysis or Sabine model can be an efficient approach. These methods assume deterministic treatment and almost nothing is known about the effect of uncertainties in the parameters, acoustic velocity and acoustic pressure inside cavities. This paper presents a study on the patterns of density and energy flow generated guide acoustic waves at high frequencies including uncertainties in geometric parameters and property of fluids. The waveguide is modelled by the Spectral Element Method Energy. The mean and variance of energy density and the flow of energy are calculated by using Monte Carlo simulation. Numerical examples show the influence of the random parameters in the different variation of the waveguide.*

Keywords: *Quantification of uncertainty, Waveguides, Spectral element method energy, Monte Carlo simulation*

1 INTRODUCTION

Currently, for design of products such as aircrafts, cars, trains household appliance, lecture rooms, and etc., acoustic comfort is a very important factor in determining whether an item is accepted or not by consumers. A number of tools is now available to aid design engineers including, Sabine room acoustic model, Modal Analysis, SEA, FEM, and Energy methods. Despite that, scientists and researchers have been developing new predictive tools that are more efficient. FEM have the inherent characteristic to generate high order computational models, which makes their use inadequate at high modal density range. Therefore, complex structure behaviour at high-frequency band is still an active research subject (Moraes *et al.*, 2009). A commonly used high frequency modelling approach is SEA (Lyon & DeJong, 1975). Its limitation comes from the inability to calculate the energy spatial variation in each subsystem. EFA is an enhanced SEA, since it provides the spatial energy distribution within the subsystems (J.C. Wohlever, 1992). The ESEM consists of applying the same matrix methodology of FEM to the analytical solution of EFA (Santos *et al.*, 2008).

During the last few years, research has been performed to deal with uncertainties in system models. The uncertainties can be linked to the geometric properties, material characteristics and boundary conditions among other possibilities. The Direct Method consists in applying the moment equations to obtain the random solutions. The unknowns are the moments and their equations are derived by taking averages over the original stochastic governing equations. Otherwise, non-sampling approaches may be used, such as the Perturbation method (Kleiber & Hien, 1992; Xiu, 2010), Neumann expansion method Yamazaki *et al.* (1988); Zhu *et al.* (1992), Moment Equations Xiu (2010), Polynomial Chaos (PC) expansion and Generalized Polynomial Chaos Ghanem & Spanos (1991); Xiu (2010), Stochastic Galerkin method Maître & Knio (2010), Stochastic Partial Differential Equations (SPDEs), and Stochastic Finite Element method Ghanem & Spanos (1991). Due to the simple process and high precision, Monte Carlo simulation has been widely used in probability and statistics analysis; MC also describes the uncertainty propagation of the input/output variables Sobol' (1994). Generally, the uncertainty parameters are assumed to follow certain forms of a probability distribution. However, an extremely large amount of iterative calculations are involved, which might affect the calculation efficiency.

In this paper the ESEM formulation for acoustic wave propagation problem in a single and coupled finite one-dimensional waveguide (duct) is presented. To turn the analysis more realistic, uncertainties are included in the gas properties and duct geometry. Such uncertainties are assumed to be spatially homogeneous along the length and Monte Carlo simulation is used to generate samples for the statistical moments analyses. The ESEM used in this work generally assumes deterministic treatment and almost nothing is known about the effect of uncertainties in the parameters, acoustic velocity and acoustic pressure inside cavities. Based on that, the novel of the paper is to study the patterns of density and energy flow generated guide acoustic waves at high frequencies including uncertainties in geometric parameters and property of fluids in a single and coupling circular cross section duct. The simulation is carried out for a single and coupling circular cross section duct using ESEM, also energy density and flow results are presented.

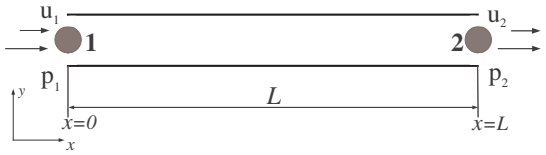

Figure 1: Two-node acoustic spectral element

2 ONE-DIMENSIONAL ACOUSTIC ENERGY SPECTRAL ELEMENT

The governing equations for acoustic and structural one-dimensional waveguides are based on the Spectral Element Method presented by Doyle (1997); Lee (2004). The Helmholtz equation is the linearised, lossless wave equation for sound propagation in fluids, re-written here as a lossy wave equation as Kinsler *et al.* (1982):

$$\frac{\partial^2 \hat{p}}{\partial x^2} - k_c^2 \hat{p} = 0, \tag{1}$$

where $\hat{}$ indicates frequency domain function, and p is the acoustic pressure. The complex wavenumber is included to account for the energy absorption mechanism in the gas, given by $k_c \approx k(1 - i\eta/2)$ with $i = \sqrt{-1}$. The linear Euler equation states the relationship between particle velocity and acoustic pressure as:

$$\hat{u} = -\frac{1}{i\omega\rho}\frac{\partial \hat{p}}{\partial x}, \tag{2}$$

where ρ is the mass density. The general solution of Eq. (1) can be written as,

$$\hat{p}\,(x) = Ae^{-ik_c x} + Be^{ik_c x}, \tag{3}$$

where A and B are constant coefficients determined from the boundary conditions.

By applying end conditions in a two-node acoustic spectral element (Fig. 1), the acoustic pressure at any arbitrary point along the element is,

$$\hat{p}\,(x) = \hat{g}_1(x)p_1 + \hat{g}_2(x)p_2 \tag{4}$$

where, $\hat{g}_1(x)$ and $\hat{g}_2(x)$ are the interpolation functions of the spectral element. By substituting Eq. (4) in Eq. (2) the particle velocity at any arbitrary point along the element can be written as,

$$\hat{p}\,(x) = \frac{1}{1 - e^{2ik_c L}}\left[\left(e^{ik_c x} - e^{ik_c(2L-x)}\right)\hat{p}_1 + \left(e^{ik_c(L-x)} - e^{ik_c(L+x)}\right)\hat{p}_2\right] \tag{5}$$

Applying end conditions in the two-node acoustic spectral element (Fig. 1), particle volumetric velocity can be written in a matrix form as:

$$\left\{\begin{array}{c}\hat{U}_1\\ \hat{U}_2\end{array}\right\} = -\frac{\mathrm{S}k_c}{\omega\rho\left(1 - e^{2ik_c L}\right)}\left[\begin{array}{cc}1 + e^{2ik_c L} & -2e^{ik_c L}\\ -2e^{ik_c L} & 1 + e^{2ik_c L} + Z_{mL}\end{array}\right]\left\{\begin{array}{c}\hat{p}_1\\ \hat{p}_2\end{array}\right\} \tag{6}$$

Assuming the duct as shown in Fig. 1 which is a duct unflanged open end, a radiation impedance (ZmL) is included in the model as demonstrated by Kinsler *et al.* (1982).

$$Z_{mL} = \rho c S\left\{\frac{1}{4}(kr)^2 + i0.6kr\right\} \tag{7}$$

where S is element section area and r is duct radius. The time-average (indicated by $\langle\rangle$) energy density in an acoustic medium is the sum of potential and kinetic energy densities as:

$$\langle e \rangle = \frac{1}{4}\left(\rho \hat{u}\hat{u}^* + \frac{1}{\rho c^2}\hat{p}\hat{p}^*\right), \tag{8}$$

Time-average energy flow (intensity) in an acoustic medium is written as:

$$\langle q \rangle = \frac{1}{2}\Re\left\{\hat{p}\hat{u}^*\right\}, \tag{9}$$

where $\Re$ is the real part of a complex number and * represents complex conjugate.

An extension of Energy Spectral Element Method (ESEM) to the acoustic medium is proposed, which allows solving the approximated energy flow solution by applying the same matrix scheme as Finite Element Method and Spectral Element Method. For steady state condition, harmonic excitation, small gas loss factor $(\eta << 1)$, the time and space averaged energy density for acoustic plane waves in a one-dimensional waveguides can be written as J.C. Wohlever (1992),

$$-\frac{c^2}{\eta\omega}\nabla^2\left\langle \bar{e}\right\rangle + \eta\omega\left\langle \bar{e}\right\rangle = \Pi \tag{10}$$

where $-$ represents space-average, e is the energy density calculated using Eq. (8), η is the gas loss factor, ω is the circular frequency, c is the sound velocity and Π is the input power. The energy flow (intensity) obtained by Eq. (9) is related to the energy density by:

$$\left\langle \bar{q}\right\rangle = -\frac{c^2}{\eta\omega}\nabla\left\langle \bar{e}\right\rangle. \tag{11}$$

The one-dimensional homogeneous solution of Eq. (10) is given by:

$$\left\langle \bar{e}\right\rangle(x) = Ge^{\eta k x} + He^{-\eta k x}, \tag{12}$$

where $k = \omega/c$ is the wavenumber, G and H are constant coefficients determined from boundary conditions. By applying end conditions in a two-node acoustic energy spectral element, the energy density at any arbitrary point along the element is obtained as:

$$\left\langle \bar{e}\right\rangle(x) = \underbrace{\left(\frac{e^{\eta k x} - e^{\eta k(2L-x)}}{1+e^{2\eta k L}}\right)}_{h_1(x)}\left\langle \bar{e_1}\right\rangle + \underbrace{\left(\frac{e^{\eta k(L-x)} - e^{\eta k(L+x)}}{1+e^{2\eta k L}}\right)}_{h_2(x)}\left\langle \bar{e_2}\right\rangle \tag{13}$$

where $h_1(x)$ and $h_2(x)$ are the interpolation functions of the energy spectral element. By substituting Eq. (13) in Eq. (11) the energy flow at any arbitrary point along the element can be written as,

$$\left\langle \bar{q}\right\rangle(x) = -\frac{kc^2}{\omega\left(1-e^{2\eta k L}\right)}\left[\left(e^{\eta k x} - e^{\eta k(2L-x)}\right)\left\langle \bar{e_1}\right\rangle + \left(e^{\eta k(L+x)} + e^{\eta k(L-x)}\right)\left\langle \bar{e_1}\right\rangle\right] \tag{14}$$

By applying end conditions in a two-node acoustic spectral energy element the energy flow can be written in a matrix form as:

$$\left\{\begin{array}{c}\left\langle \bar{q_1}\right\rangle \\ \left\langle \bar{q_2}\right\rangle\end{array}\right\} = -\frac{kc^2}{\omega\left(1-e^{2\eta k L}\right)}\left[\begin{array}{cc}1+e^{2\eta k L} & -2e^{\eta k L} \\ -2e^{\eta k L} & 1+e^{2\eta k L}\end{array}\right]\left\{\begin{array}{c}\left\langle \bar{e_1}\right\rangle \\ \left\langle \bar{e_2}\right\rangle\end{array}\right\} \tag{15}$$

Reactive-type exhaust mufflers use the ability of a cross section area change to attenuate the sound energy transmitted in a duct. Also, the medium property change in a duct will attenuate the sound energy transmitted. In the acoustic filter theory, the medium is assumed to be stationary and the wave propagation is governed by the 1-D wave equation. To account for these discontinuities in the energy model, additional coupling relationships need to be formulated and inserted at these connection points. Since a rod and an acoustic duct are ruled by the same wave equation, the joint element used in this study is the same proposed by Cho & Bernhard (1998) for structural coupling type rod-rod. Then, the acoustic coupling relationship is obtained as:

$$\left\{ \begin{array}{c} \langle \bar{q_1} \rangle \\ \langle \bar{q_2} \rangle \end{array} \right\} = -\frac{\tau_{ij}}{2r_{ij}} \left[\begin{array}{cc} c_i & -c_j \\ -c_i & c_j \end{array} \right] \left\{ \begin{array}{c} \langle \bar{e_1} \rangle \\ \langle \bar{e_2} \rangle \end{array} \right\} \tag{16}$$

where τ_{ij} and r_{ij} are the power transmission and reflection coefficients at the coincident nodes between elements i and j. The radiation impedance is included in the ESEM as $\langle q \rangle = \alpha c \langle e \rangle$, where $\alpha = \tau/(2-\tau)$ and $\tau = 1 - |(Z_{mL} - \rho c)/(Z_{mL} + \rho c)|2$. Specifically, impedance radiation (Z_{mL}), is the term that accounts for the change in geometry or medium properties.

3 MONTE CARLO SIMULATION

The Monte Carlo simulation has been used for decades, it is a method based on random samples used in approximations. The name itself is taken from the famous casino located in Monte Carlo (Sampaio & Lima, 2012). Simulation methods are also named exact methods, because the simulation result leads to exact outcomes when the sample number goes to infinity. To avoid certain approximations which occur in analytical methods and to be a non-intrusive method are another advantages of this type of techniques. Thus, the general idea of the method is solving mathematical problems by the simulation of random variables (Sobol', 1994). An Monte Carlo method example of application is the multidimensional integral approximation. Supposing the integral of a given real multidimensional function g in a certain region $B \subset \mathbb{R}$,

$$I = \int_B g(\mathbf{x}) d(\mathbf{x}) \tag{17}$$

If g is a simple function, its integral (I) can be calculated easily. However, if g is a difficult function or is defined in a region with complicated contour, it may not exist a closed form for (I). In such cases, numerical integration methods must be applied in order to obtain approximations for (I), such as the trapeze method, Simpson method and Monte Carlo simulation. Assuming that (I) is a one-dimensional integral, p a function density probability of a random variable $\mathbf{X}$, rewriting Eq. (17) gives,

$$I = \int_B h(\mathbf{x}) p(\mathbf{x}) d(\mathbf{x}) \tag{18}$$

where $h(\mathbf{x}) = g(\mathbf{x})/p(\mathbf{x}) \forall \mathbf{x} \in B$. The integral I can be interpreted as the expected value of $h(\mathbf{x})$, it is:

$$I = \mathbb{E}[h(\mathbf{x})] = \int_B h(\mathbf{x}) p(\mathbf{x}) d(\mathbf{x}) \tag{19}$$

Thus, an approximation $(\hat{I})$ for the integral can be expressed as

$$\hat{I} = \sum_{i=1}^{n} h(\mathbf{x}^i) \tag{20}$$

where $x(1), x(2), ..., x(n)$ are samples of the random vector $\mathbf{X}$ with probability density function p.

The mean and the standard deviation of the result are calculated through the samples generated. Let $X(\xi, \omega)$ be the frequency response of the stochastic system calculated for a realization ξ, generated by the Monte Carlo method Rubinstein (2008).

4 SIMULATION RESULTS

4.1 Single duct

The one-dimensional acoustic waveguide consists of a rigid wall cylindrical duct with an unflanged open end and harmonically excited at the other end as illustrated in Fig. (2). The acoustic medium is the air at $20°C$ ($\rho = 1.21$ kg/m^3; $c = 343$ m/s; and $\eta = 2.86 \times 10^{-3}$), and the duct geometry is $S = 2.0^{-3}$ m^2 and $L = 6.0$ m. The harmonic excitation applied at node 1 for the ESEM model is the corresponding input power calculated with the Eq. (9) at the frequency $f = 500\,\mathrm{Hz}$. By computing the statistic moments of energy density and energy flow the mass density (ρ) and duct length (L) are assumed to be spatially homogeneous Lognormal random variables with coefficient of variation (COV) of 2 and 10%. The first and second statical moments are calculated using the non-intrusive Monte Carlo simulation method with 500 samples.

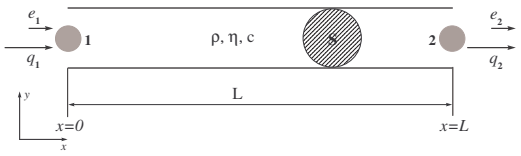

Figure 2: Two-node one-dimensional acoustic waveguide element for single duct.

Figures. (3(a)) and (3(b)) demonstrate separately the influence of the variability in mass density (ρ) and duct length (L), with COV of 10% respectively. The mean and standard deviation (envelope) of the energy density is compared with deterministic result.The mean of the energies density are found closely follow the deterministic results. It is visible that variability in ρ is more sensible than in L when the energies density amplitude is analysed. The parameters sensibility analyse in the energy density with variability in both parameters are shown in Fig. (3(c)). Similar behaviour of the Fig. (3(b)) is observed in this cases.

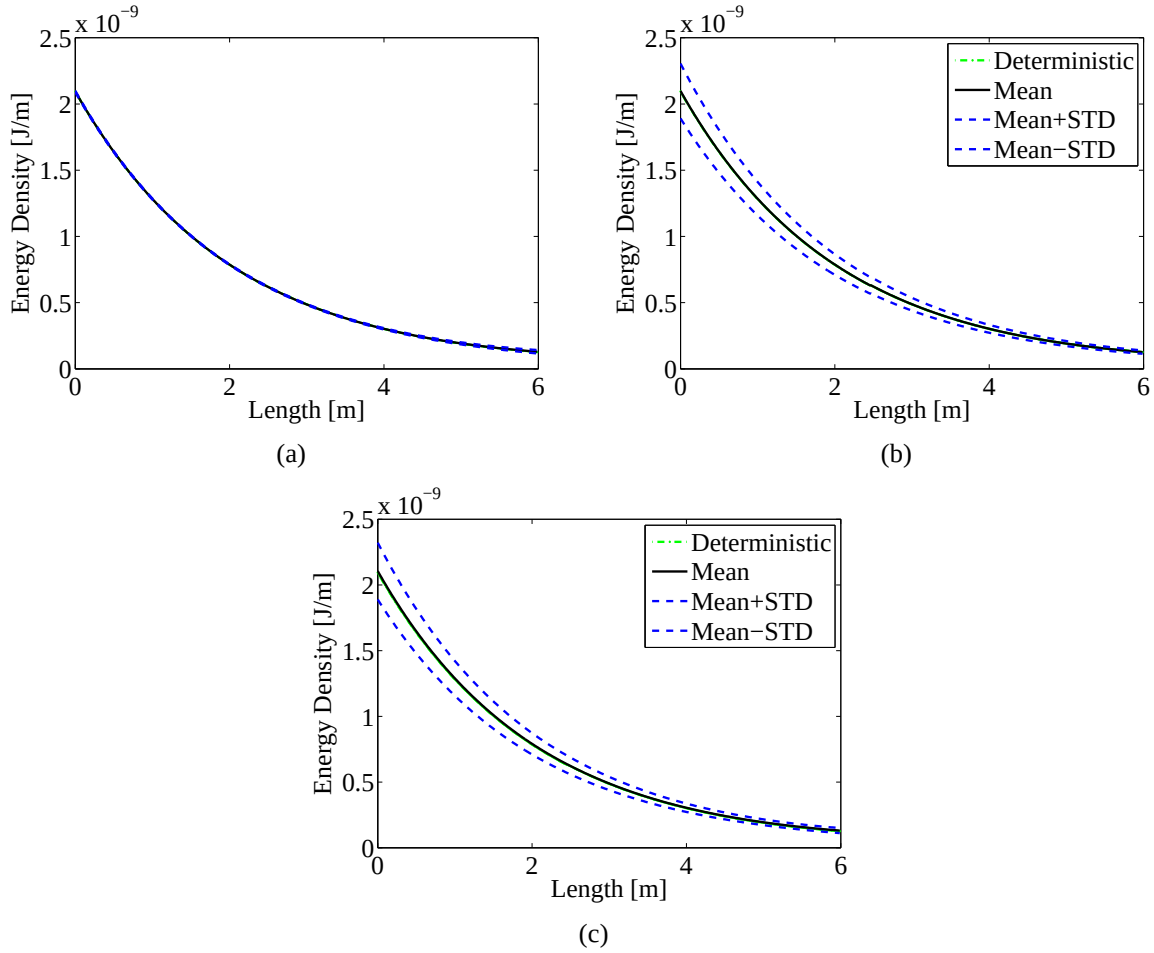

Figure 3: Mean, standard deviation and deterministic energy density for a single duct with L (a), ρ (b) and both (L,ρ) (c) as random variable.

In the case of the flow energy also the variability in mass density (ρ) and duct length (L), with COV of 10% were analysed (Fig. 4). As in density energy, the flow energy mean is close to the deterministic results. The standard deviation (envelope) is more evident with the variance of (ρ) than (L). The correspondent behaviour of the Fig. (4(c)) was obtained. In this type of system, the mass density is directly affected by the air temperature, based on the presented results a strict temperatures control should be done. In the single duct density and flow energy presented close behaviour. Figures. (5) and (6) show the (ρ) and (L) variability influence in density and flow energy estimation for different COV's (2% and 10%). The mean energies with COV's of 2% and 10% follow the deterministic result, and the standard deviation (envelope) demonstrate the variability in these both case. As commented, the temperature control which implies in mass density variability is essential in this type of system. The behavior can be seen in Figs. (5 and 6). For small COV the variability in the energies is close to mean response while that for high COV the envelope increase, especially between 0 to 2 m in the duct length. It because the energy is more intense at the node 1 (excitation point), after that the energy decrease in reason of the damping effect.

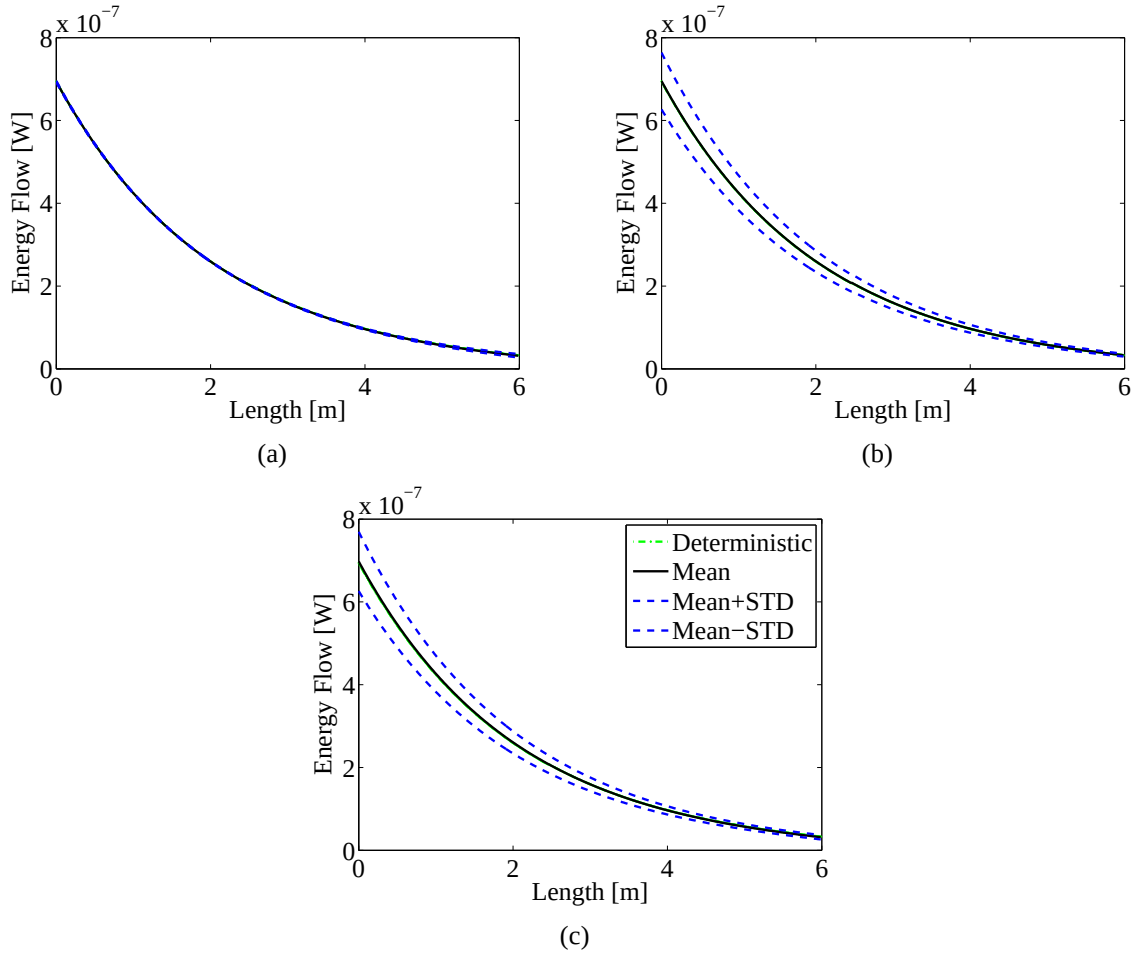

Figure 4: Mean, standard deviation and deterministic flow energy for a single duct with L (a), ρ (b) and both (L,ρ) (c) as random variable.

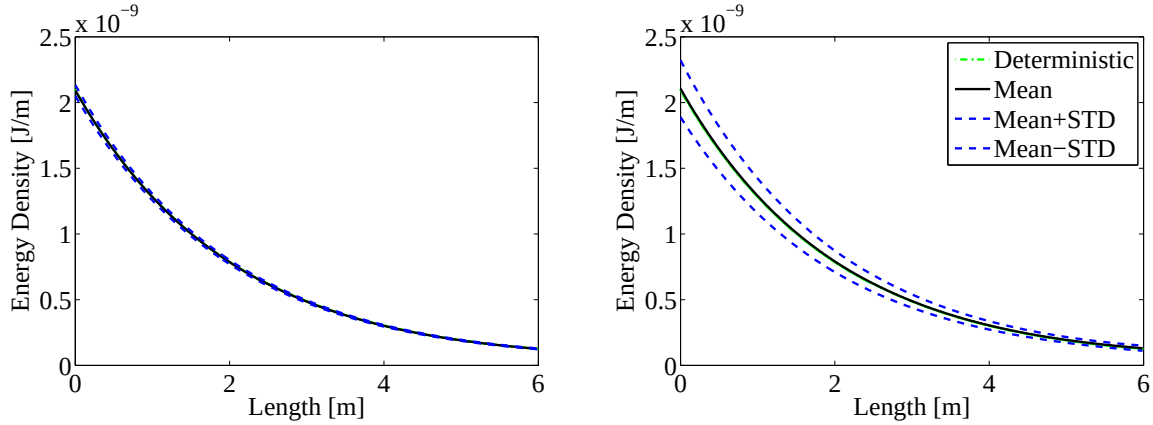

Figure 5: Energy density for a single duct with COV of 2% (left-hand side) and 10%(right-hand side).

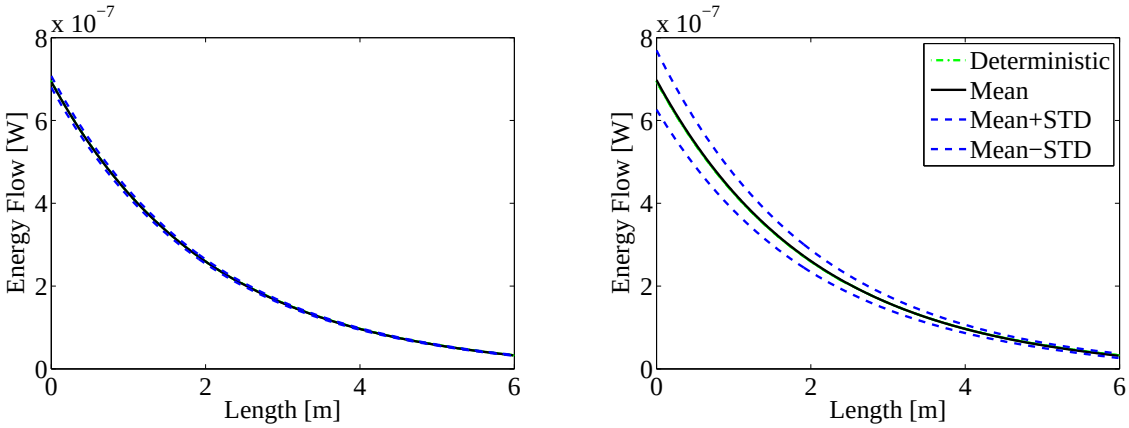

Figure 6: Flow energy for a single duct with COV of 2% (left-hand side) and 10%(right-hand side).

4.2 Coupled duct

The coupled acoustic system consists of two one-dimensional acoustic waveguide (rigid wall ducts) with different geometry (cross section radius and length) or medium property (sound velocity, gas density and loss factor) connected each other, as showed in Fig. (7). The system is harmonically excited at the left end and opened in the right end (unflanged). For the geometric discontinuity the duct dimensions for element 1 are $S_1 = 2.0 \times 10^{-3}$ m and $L_1 = 1.8$ m, while for element 2 are $S_2 = 4.0 \times 10^{-3}$ m^2 and $L_2 = 4.2$ m. Both elements contains air at $0°C$ ($\rho = 1.21$ kg/m^3; $c = 343.0$ m/s; and $\eta = 5.8 \times 10^{-3}$) as acoustic medium. For the medium discontinuity the element 1 contains air at $0°C$ (ρ_1=1.293 kg/m^3, $c_1 = 331.6$ m/s, $\eta_1 = 5.8 \times 10^{-3}$), while the element 2 contains hydrogen at $0°C$ ($\rho_2 = 0.09$ kg/m^3; $c_2 = 1269.5$ m/s; and $\eta_2 = 8.810^{-3}$). Both elements have same geometric dimensions ($S = 5.0 \times 10^{-3}$ m^2 and $L = 6$m). The excitation and end conditions are the same as the single element problem, but the frequency-averaged energy density and flow responses were calculated by ESEM in 1/3-octave frequency band with center frequency $f_c = 8$ kHz .

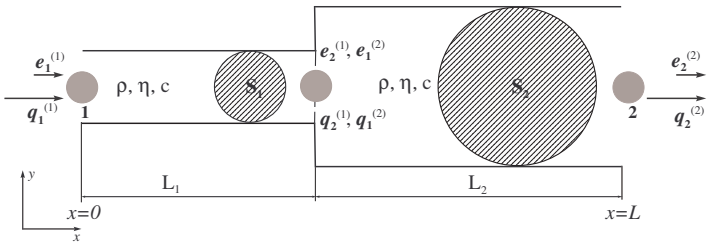

Figure 7: Two-node one-dimensional acoustic waveguide element for coupling duct.

Likewise the analyses realized for the single duct, Figs. (8(a)) and (8(b)) show the influence of the variability of 10% in mass densities (ρ and ρ_2) and duct length (L) with section variation. The coupling duct, with cross section area discontinuity, causes an energy decay at the discontinuity position(L_1). When the duct length is assumed as a random variable (L_1 is related to the duct length), the density energy decay presented a variability at discontinuity position. Figure. (8(a)) shows mean and standard deviation (envelope) of the energy density compared deterministic results. For the mass densities (ρ and ρ_2) assumed as a random variable

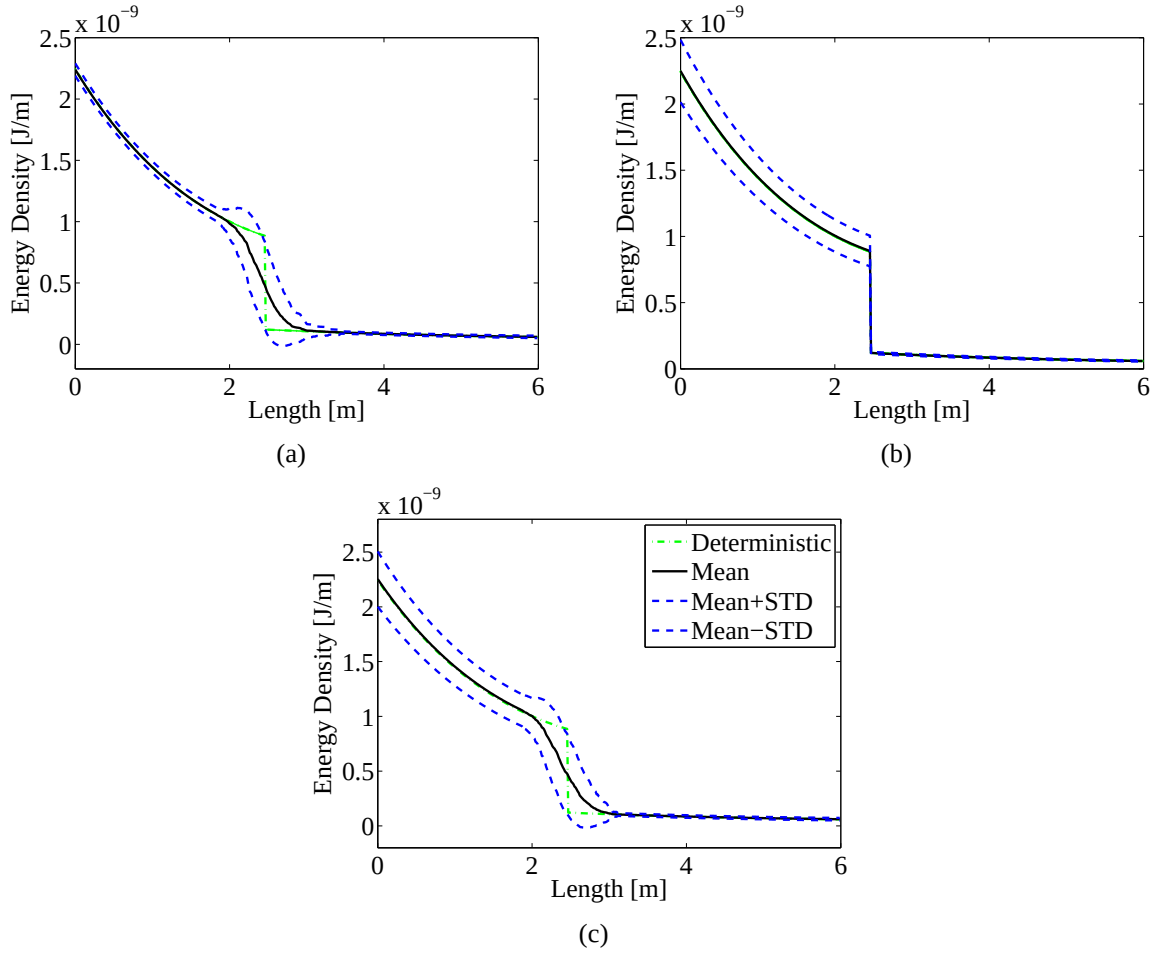

Figure 8: Mean, standard deviation and deterministic energy energy for a coupling duct with L (a), ρ (b) and both (L,ρ) (c) as random variable.

the amplitude until the discontinuity position presented a variation, while the position indeed shows significant changes. Figure. (8(b)) shows the comparison of mean, standard deviation (envelope), and deterministic energy density with mass densities variation. Interesting results can be seen in Figure. (8(c)) which illustrates mean and standard deviation (envelope) of the energy density compared with a deterministic result. In this case, duct length and both mass densities were assumed to be a random variable. An influence of the combination behavior when the variability in all parameters (L, ρ, ρ_2) is presented. Different of the single duct, now the mass densities and duct length should be strict control in a way to localize the discontinuity position.

Figures (9(a))- (9(c)) show the (ρ and ρ_2) and (L) variability influence in the flow energy estimation for COV of 10%. A light decay can be observed in the flow energy with the change section. The mean and standard deviation flow energy are very close to deterministic result when L is random. An amplitude variation is higher between 0 to 2m when ρ and ρ_2 are the random variable in reason of the high energy at the node 1 and the damping consequence. the combination of the behavior when ρ, ρ_2 and L are assumed the random variable is demonstrated in fig. (9(c))

Figures (10) and (11) show the (ρ and ρ_2) and (L) variability influence in density and

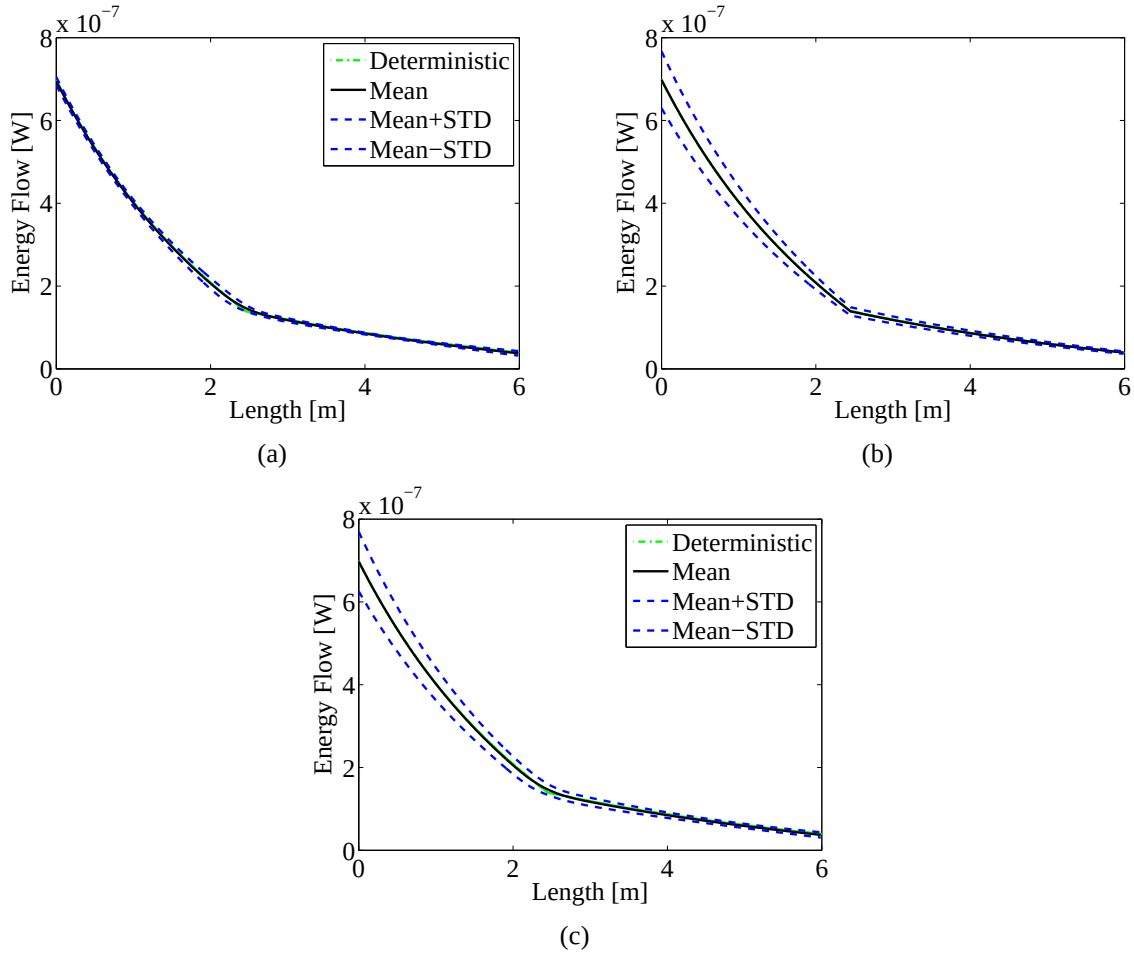

Figure 9: Mean, standard deviation and deterministic flow energy for a coupling duct with L (a), ρ (b) and both (L,ρ) (c) as random variable.

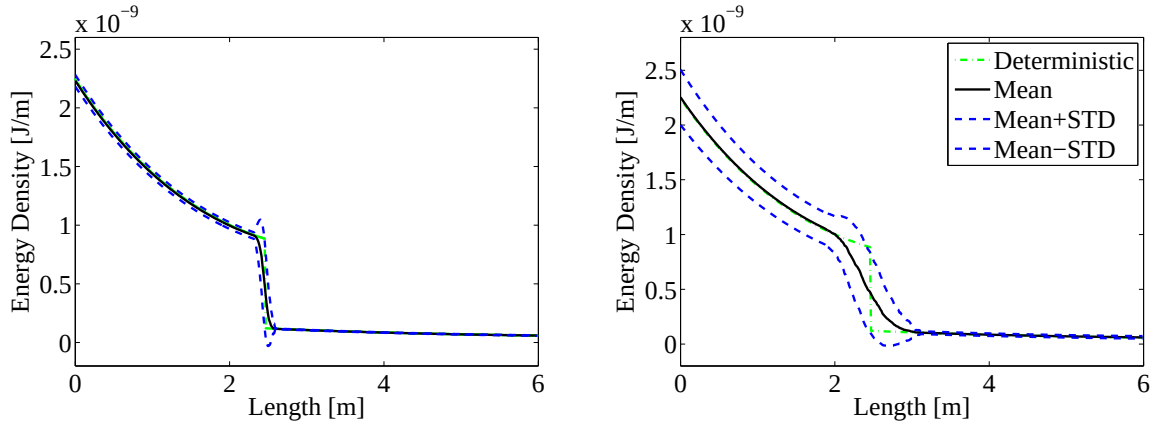

Figure 10: Energy density for a coupling duct with COV of 2% (left-hand side) and 10%(right-hand side).

flow energy estimation for different COV's of 2% and 10%. In those case, mass density and duct length induce a dispersion at the discontinuity position. As the single duct analyse, for small COV the variability in the energies is close to mean response while that for high COV the envelope increase, especially between 0 to 2 m in the duct length.

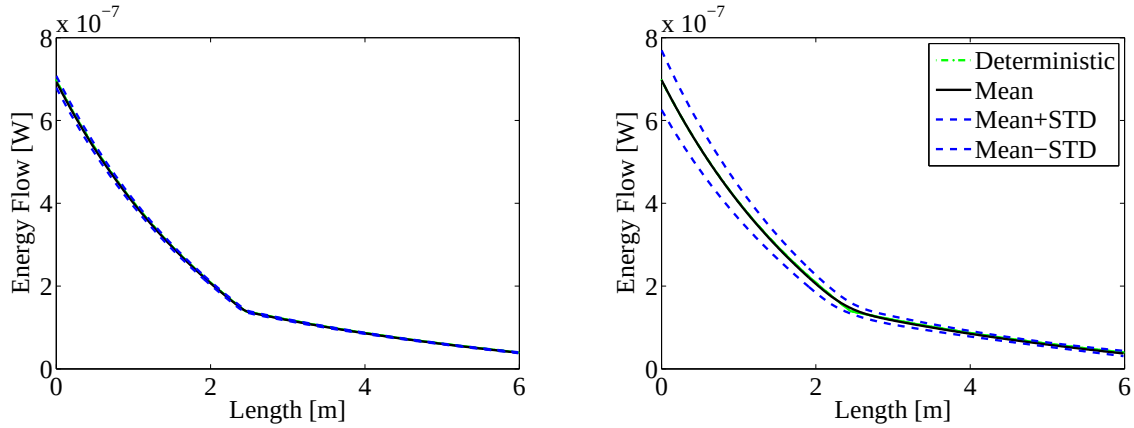

Figure 11: Flow energy for a coupling duct with COV of 2% (left-hand side) and 10%(right-hand side).

5 CONCLUSION

The novel of the paper is to study the patterns of density and energy flow generated guide acoustic waves at high frequencies including uncertainties in geometric parameters and property of fluids in a single and coupling circular cross section duct. The ESEM formulation for acoustic wave propagation problem in a single and coupled finite one-dimensional waveguide (duct) with a spatially homogeneous uncertainty parameter is presented. To handle with this random parameter, the Monte Carlo simulation is used to generate samples for the statistical moments analyses. Interesting behaviors were observed for a single and coupling duct. In the single duct density and flow energy presented close behavior. Mass density is shown more sensible than duct length,the mean energies with COV's of 2% and 10% follow the deterministic result, and the standard deviation (envelope) demonstrate the variability in these both case. For small COV the variability in the energies is close to mean response while that for high COV the envelope increased. However it was observed and great energy variation close to the node 1 (excitation point), and a damping effect along the duct. In a coupling duct with cross section area discontinuity causes an energy decay at the discontinuity position(L_1). Both parameters, duct length and mass density showed sensitive, it was more evident in the energy density. In this case, mass densities and duct length should be strict control in a way to localize the discontinuity position.

ACKNOWLEDGEMENTS

The authors are grateful to the government research funding agencies Fundação de Apoio à Pesquisa do Estado do Maranhão - FAPEMA, Fundação de Amparo à Pesquisa do Estado de São Paulo - FAPESP, Conselho Nacional de Desenvolvimento Científico e Tecnológico - CNPq, Fundação de Amparo à Pesquisa do Estado de Minas Gerais - FAPEMIG and Coordenação de Aperfeiçoamento de Pessoal de Nível Superior - CAPES for the financial support for this work.

REFERENCES

Cho, P.E., & Bernhard, R.J. 1998. Energy flow analysis of coupled beams. *Journal of Sound and Vibration*, **211**, 593–605.

Doyle, James F. 1997. *Wave Propagation in Structures: Spectral Analysis Using Fast Discrete Fourier Transforms*. New York: Springer-Verlag.

Ghanem, R., & Spanos, P. 1991. *Stochastic Finite Elements - A Spectral Approach*. Sprin.

J.C. Wohlever, R.J. Bernhard. 1992. Mechanical energy flow models of rods and beams. *Journal of Sound and Vibration*, **153**, 1–19.

Kinsler, Lawrence E., Frey, Austin R., Coppens, Alan B., & Sanders, James V. 1982. *Fundamentals of Acoustics*. John Wiley & Sons.

Kleiber, M., & Hien, T.D. 1992. *The Stochastic Finite Element Method*. John Wiley.

Lee, U. 2004. *Spectral Element Method in Structural Dynamics*. New York: Springer-Verlag.

Lyon, Richard H., & DeJong, Richard G. 1975. *Theory and Application of Dynamics Systems, Second edition*. Boston: Butterworth-Heinemann.

Maître, O.P. Le, & Knio, O.M. 2010. *Spectral methods for uncertainty quantification*. Springer.

Moraes, E. C., Pereira, V. S., & Dos Santos, J. M. C. 2009. Energy spectral element method for acoustic waveguides. *In:* ABCM (ed), *Proceedings of PACAM XI*.

Rubinstein, R. Y. 2008. *Simulation and the Monte Carlo Method, 2nd Edition*. Wiley.

Sampaio, R., & Lima, R. 2012. *Modelagem Estocástica e Geração de Amostras de Variáveis e Vetores Aleatórios*. SBMAC (Notas em Matemática Aplicada; v. 70).

Santos, E.R.O., Arruda, J.R.F., & Santos, J.M.C. Dos. 2008. Modeling of coupled structural systems by an energy spectral element method. *Journal of Sound and Vibration*, **36**, 1 – 24.

Sobol', I. M. 1994. *A primer for the Monte Carlo method*. CRC Press.

Xiu, D. 2010. *Numerical Methods for Computations-A Spectral method approcah*. Princeton University Press.

Yamazaki, F., Shinozuka, M., & Dasgupta, G. 1988. Neumann expansion for stochastic finite element analysis. *Journal Engineering Mechanics-ASCE*, **114 (8)**, 1335–1354.

Zhu, W.Q., Ren, Y.J., & Wu, W.Q. 1992. Stochastic FEM based on local averages of random vector fields. *Journal Engineering Mechanics-ASCE*, **118 (3)**, 496–511.